

Fabrication and Characterization of Organolead Halide Perovskite Solar Cell

Mahdi Hasan Suhail¹ and Aqel Mashot Jafar²

¹Physics Department, College of Science, University of Baghdad, Ministry of Higher Education and Scientific Research, Baghdad, Iraq.

²Solar Energy Research Center, Renewable Energy Directorate, Ministry of Higher Education and Scientific Research, Baghdad, Iraq.

ARTICLE INFO

Article history:

Received: 12 August 2016;

Received in revised form:

14 September 2016;

Accepted: 24 September 2016;

Keywords

Perovskite solar cells,
Organolead halide,
Optical properties,
Methyl-ammonium Iodide,
CuI .

ABSTRACT

This research presents the description of the procedure for the manufacturing the Organolead halide Perovskite Solar Cells (OPSC). We described the synthesis organolead halide perovskite materials, MAPbI₂Br and MAPbBrCl₂, which employed as absorption layer in OPSCs . Optical properties for the perovskite materials which used to prepare OPSCs is tested by the measurements the absorbance spectrum in order to calculate the energy gap . X-ray diffraction, AFM microscope and SEM microscope are used in our work to study the structure of the samples. Finally, the tests OPSCs by Light I-V Measurement System are implemented in order to obtain the parameters of the manufacturing devices. The Power Conversion Efficiencies (PCE) of OPSCs are (0.12%) and (0.07%) to the devices have MAPbI₂Br and MAPbBrCl₂ as sensitized absorption layer, respectively. Measurements are tested at AM1.5 global sunlight (100 mW cm⁻²) .

© 2016 Elixir All rights reserved.

Introduction

Global energy consumption has been continually increasing with population growth and fast-paced industrial development in recent decades, which demands renewable energy sources in view of long-term sustainable development. Generating cost-effective and environmentally benign renewable energy remains a major challenge for both technological and scientific development . Solar cells based on the photovoltaic with the advantages of decentralization and sustainability have attracted great attention in the past 50 years. Currently, the photovoltaics markets is dominated by crystalline silicon-based solar cells with a share of 89% ; however, a cost-effective and high-throughput material named perovskite has proven to be capable of Power Conversion Efficiency (PCE) 20%[1] , compared to 3.8% [2] of PCE that was obtained only four years ago . Organic-inorganic halide perovskite solar cells have been the most significant development in the field of photovoltaic's in the present decade and are the best bet at satisfying the need for high efficiencies while allowing for low cost solution based manufacturing . Low cost , stability and high efficiency are research reason in the development of organic-inorganic perovskite solar cells. Organolead halide perovskite solar cells has attracted researchers attention as a light harvester for perovskite solar cells because of its tenable band gap, large absorption coefficient, high charge carrier mobility, and long electron-hole diffusion [3,4] .

Basic Theory

Perovskites materials are described by the formula ABX₃, where X is an anion and A and B are cations of different sizes (A being larger than B). The "A" cation is divalent and the "B" cation is tetravalent . In the cubic unit cell, the A-cation resides at the eight corners of the cube, while the B-cation is

located at the body center that is surrounded by 6 X-anions (located at the face centers) in an octahedral [BX₆]⁻⁴ cluster [5].The crystal structure of perovskites is depicted in Fig.1[6].

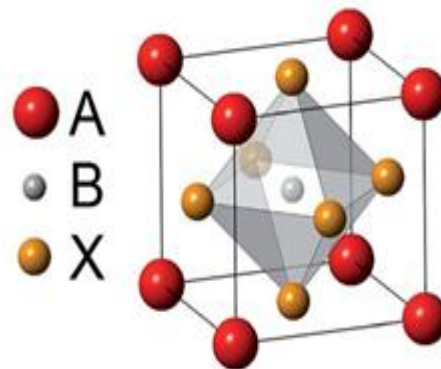


Fig 1. Inset depicts schematic to the perovskite structure [6].

The PCE of solar cell device is estimated by the equation (1) [6-8]:

$$PCE = \frac{FF * V_{oc} * I_{sc}}{P_{in} * A_{ac}} \quad (1)$$

Where FF, V_{oc} , I_{sh} , P_{in} and A_{ac} are full factor , open voltage circuit ,short current circuit , input power to the solar cell estimated to one solar illumination which equate to (100 mW/cm²) and active area of solar cell , respectively .

The optical band gap of the thin film have been investigated for the allowed direct transition from the equation (2)[6,9].

$$\alpha h\nu = B * [h\nu - E_g]^{1/2} \quad (2)$$

Where, h is the Planck constant, α is the absorption coefficient, ν is the light frequency, E_g is the optical energy gap and B is empirical constant

Experimental

Composition and crystal structure studied by X-Ray Diffraction (XRD Shimadzu 6000, Cu-K α) for USP coating. The surface morphology of sample is studied by investigation of Atomic Force Microscopy (AFM) (AA3000 Scanning probe microscope, Angstrom Advanced Inc.). The difference in the shape of the perovskite crystals studied by images of Scanning Electron Microscope (SEM) (Bruker Nano GmbH, Germany), analysis is performed by using a magnification 1kx and 5kx, high voltage 5kV and SEM in secondary electron mode.

Light I-V Measurement Test Reports are recorded by Photovoltaic measurements system, composed of Oriel I-V test station using an Oriel Solar simulator. The solar simulator is class AAA for spectral performance, uniformity of irradiance, and temporal stability. The solar simulator is equipped with a 450 W xenon lamp. The output power is adjusted to match AM1.5 global sunlight (100 mW cm^{-2}).

I-V curves are obtained by applying an external bias to the cell and measuring the generated photocurrent with a Keithley model 2400 digital source meter. The transmittance of coated films is measured in the wavelength range of (400 - 800) nm using a (SPECTRO UV/Vis Double Beam (UVD-3500) Labomed, Inc). A blank sample of substrate is used as a reference in the measurement of optical transmittance.

Synthesis of Organic Perovskite Materials (OPM) reported in Ref [6,8]. Methylamine Iodide ($\text{CH}_3\text{NH}_3\text{I}$) is prepared by reacting Methylamine, 33 wt % in Ethanol (BDH-LTD), with Hydro-Iodic acid (HI) 57 wt % in water (BDH-LTD) under ice bath stirring for 2 h. Typical quantities employed are 24 ml of Methylamine, 10 ml of HI, and 100 mL of Ethanol. Upon drying at 100°C , a white powder is formed, which is placed overnight in a vacuum oven before use. Methylamine Bromide is prepared at the same method and previous quantities. To obtain the perovskite solution precursor of MAPbBr_2 , we dissolved both the $\text{CH}_3\text{NH}_3\text{I}$ and the PbBr_2 (BDH-LTD) in anhydrous N, N-Di Methyl Formamide (DMF) (Sigma Aldrich) at a 3:1 molar ratio. To obtain the perovskite solution precursor of MAPbCl_2 , we dissolved both the $\text{CH}_3\text{NH}_3\text{Br}$ and the PbCl_2 (BDH-LTD) in anhydrous N, N-Di Methyl Formamide (DMF) (Sigma Aldrich) at a 3:1 molar ratio, with final concentrations of 40 wt %. 10 ml of solutions preparation added to 0.15 g of Nano particle > 30 nm of Al_2O_3 powder (China of origin) to obtain scaffold perovskite precursor solution of $\text{CH}_3\text{NH}_3\text{IPbBr}_2$ and scaffold perovskite precursor solution of $\text{CH}_3\text{NH}_3\text{BrPbCl}_2$.

TiO_2 compact layer preparation is a first fabricated applying Aerosol Assisted Chemical Vapor Deposition (AACVD) technique [6,8,9] by using Ultrasonic Atomizer (402AI) with ultrasonic frequency (1.5MHz). The precursor solution, which preparation of Nano particle > 20 nm of TiO_2 powder (China of origin) dispersed in ethanol solvent, is sprayed on pre-heated Transparent Conductive Oxide (TCO) glass substrates of Fluorine-doped Tin Oxide (FTO) (Coated Sodaline float glass of Visiontek, sheet Resistance $8 \Omega/\square$) at 450°C . Deposited time is 1h and the substrates are left to cold at room temperature, followed by, depositing scaffold perovskite precursor solution of $\text{CH}_3\text{NH}_3\text{IPbBr}_2$ or $\text{CH}_3\text{NH}_3\text{BrPbCl}_2$, by spin coated at speed 2000 rpm and annealing at 150°C to obtain 2 samples of (FTO/Compact TiO_2 /Scaffold $\text{CH}_3\text{NH}_3\text{IPbBr}_2$ or $\text{CH}_3\text{NH}_3\text{BrPbCl}_2$), as shown

in figure 2. The temperature of the (FTO/Compact TiO_2) coated substrates is monitored by an infrared temperature indicator through the all experimental runs.

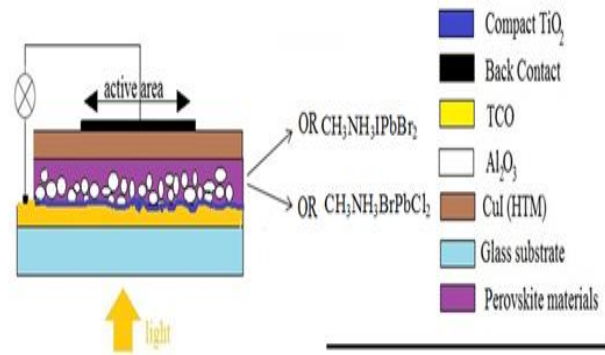
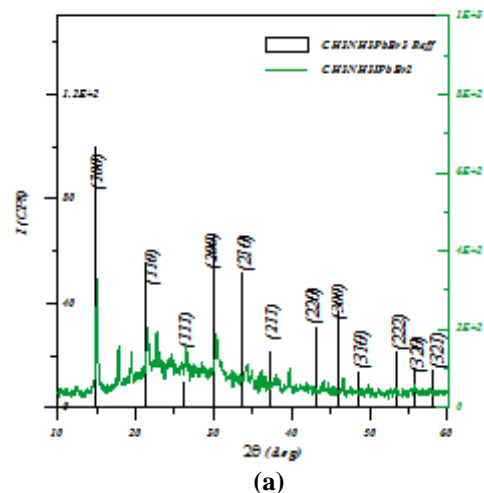


Fig (2). Inset depicts schematic 2 samples of OPSCs have different perovskite materials.

CuI thin films are deposited onto (FTO/Compact TiO_2 /Scaffold $\text{CH}_3\text{NH}_3\text{X}_3$) as a Hole Transport Layer (HTL) at room temperature by sputtering of pure CuI target in argon gas using DC sputtering technique as reported in ref [6]. In these technique, CuI target (99.99 % pure) with dimensions 50 mm diameter and 3 mm thickness is used for the sputtering. The sputter chamber is evacuated by employing diffusion pump and rotary pump combination to achieve base pressure of 3.1×10^{-5} mbar. Argon of 99.99 % purity is used as reactive and sputtering working pressure of gases of 3.2×10^{-1} mbar for deposition of the films. The argon gas flow average is 240 Scm, the 1.8 kV voltage is supplied to the sputter target using DC power supply, the discharge current of sputtering is 17.5 mA, the time of sputtering target is 1 h and active electrode spacing is 4cm. For the counter electrode, thin film of Al with 200nm-thickness deposited on top HTL by a thermal evaporation, where Al evaporated under 10^{-5} mbar vacuum condition.

Results and Discussions

The sample of the mixed halide perovskite structure $\text{CH}_3\text{NH}_3\text{BrPbI}_2$ film is appeared the peaks of XRD at reflection positions (100), (110), (111) and (200) corresponding with the cubic $\text{CH}_3\text{NH}_3\text{PbBr}_3$ structure which indicated by ref [10] as shown in fig 3(a). XRD patterns of the perovskite structure of $\text{CH}_3\text{NH}_3\text{PbBrCl}_2$ sample is exhibited the cubic $\text{CH}_3\text{NH}_3\text{PbBr}_3$ phase and can be confirmed by reflections positions of (100), (110), (111), (200) and (210) [10].



(a)

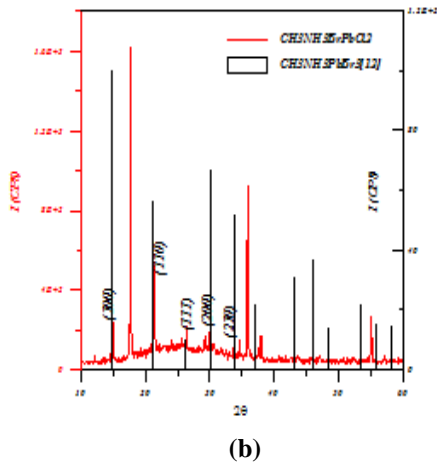


Fig 3. (a) XRD patterns of $\text{CH}_3\text{NH}_3\text{IPbBr}_2$ layer on sheet glass substrate sample comparative with $\text{CH}_3\text{NH}_3\text{PbBr}_3$ Ref [10] . (b)XRD patterns of $\text{CH}_3\text{NH}_3\text{BrPbCl}_2$ layer on sheet glass substrate samples comparative with $\text{CH}_3\text{NH}_3\text{PbBr}_3$ Ref [12].

Fig. 4 (a and b) are illustrated top SEM images of $\text{CH}_3\text{NH}_3\text{PbIBr}_2$ layer. (c and d) are top SEM images of $\text{CH}_3\text{NH}_3\text{PbBrCl}_2$ layer . Scale bars of the (a and c) images are $10\mu\text{m}$ and the (b and d) images are $5\mu\text{m}$, scanning with high voltage 5kV and magnification (5 and 10) kx , respectively. Samples are prepared by spin coated at speed 2000 rpm deposition of perovskite precursor solution on preheated sheet glass substrate at 150 C .

Fig. 4(e and f) depicts SEM images of compact layer of TiO_2 on FTO electrode deposited by (AACVD) technique on preheated sheet glass substrate at 450 C temperature and deposited at 1h time .The particle size dimensions of TiO_2 compact layer are appeared in SEM image as shown in the Fig. 4(e) , ($X=93.75\text{nm}$, $Y=93.32\text{nm}$, $D=132.3\text{nm}$) .

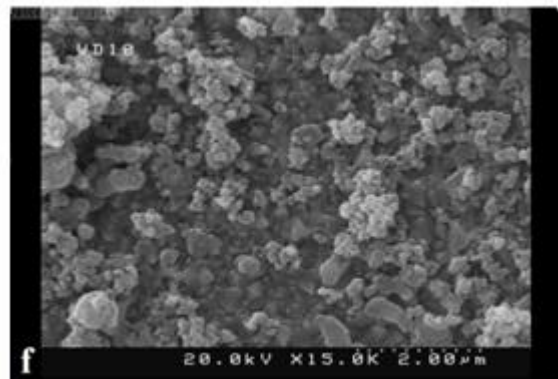
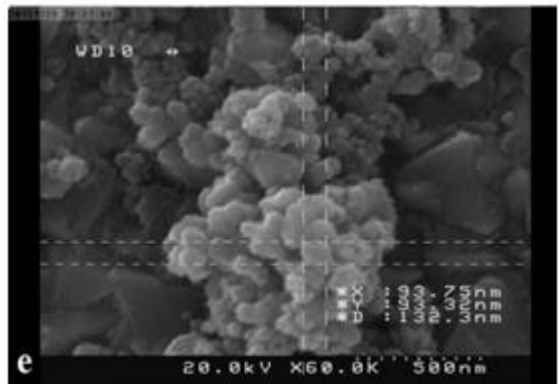
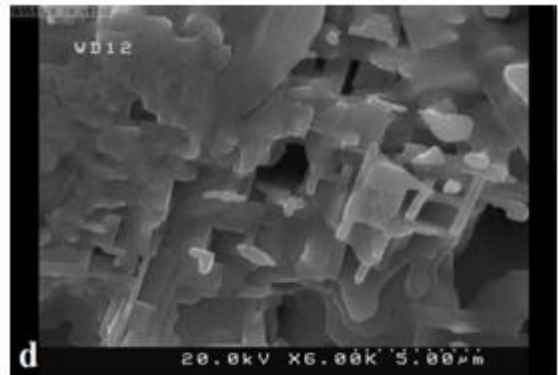
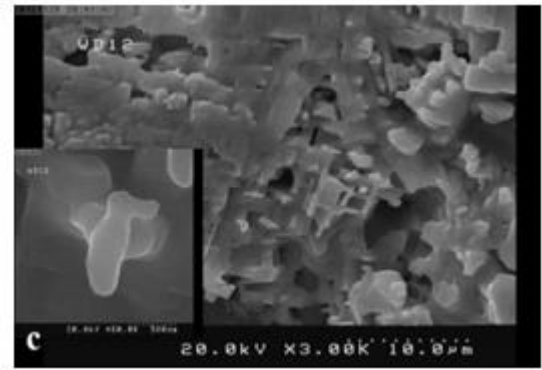
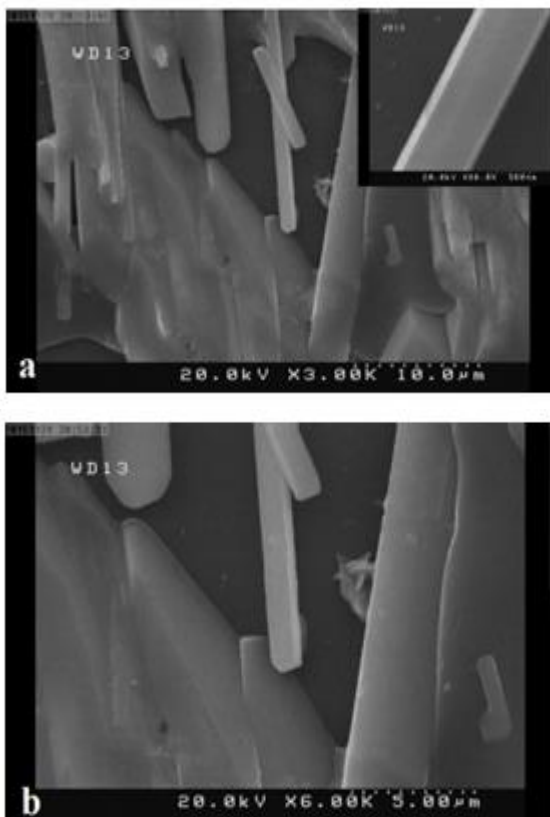


Fig 4a & b. Top SEM images of $\text{CH}_3\text{NH}_3\text{IPbBr}_2$ layer. c&d Top SEM images of $\text{CH}_3\text{NH}_3\text{BrPbCl}_2$ layer, scale bars of left perovskite images are $10\mu\text{m}$ and right images are $5\mu\text{m}$. Top SEM images of compact layer of TiO_2 on FTO electrode , Scale bar of left image is 500nm and right image is $2\mu\text{m}$.

Fig.5a is explained the absorption of halide perovskite films and appeared more absorption to $\text{CH}_3\text{NH}_3\text{IPbBr}_2$ than $\text{CH}_3\text{NH}_3\text{BrPbCl}_2$ sample that which are measured in the wavelength range (400-800) nm using a (SPECTRO UV/VIS Double Beam (UVD-3500) Labomed, Inc.) and glass substrates as reference samples. Plots inset of $(\alpha h\nu)^2$ versus photon energy ($h\nu$) for perovskite layers on glass

substrates are illustrated in Fig.9b . A direct optical band gap energy (E_g) for halide perovskites materials $CH_3NH_3X_3$, ($X = Cl, Br, I$) is reported by Simon et al [11,12]. (E_g) of samples is determined by fitting the absorption data to the direct transition equation (2). The optical band gap value is obtained by extrapolating the linear part of the curve $(\alpha hv)^2$ as a function of photon energy, $h\nu$, intercept the $(h\nu)$ axis at $\alpha = 0$. The values estimated of E_g are (1.8 and 1.92) eV for $CH_3NH_3IPbBr_2$ and $CH_3NH_3BrPbCl_2$ samples, respectively. We observed that the energy gap is decreased and the absorption is increased of the mixed halide, $X = Br$ and I , perovskite structure of $CH_3NH_3IPbBr_2$ sample, when insertion Chlorine instead of Iodine in mixed of halide, $X = Br$ and Cl , of $CH_3NH_3BrPbCl_2$ sample then the energy gap is increased and the absorption is decreased, as shown in figure 5 .

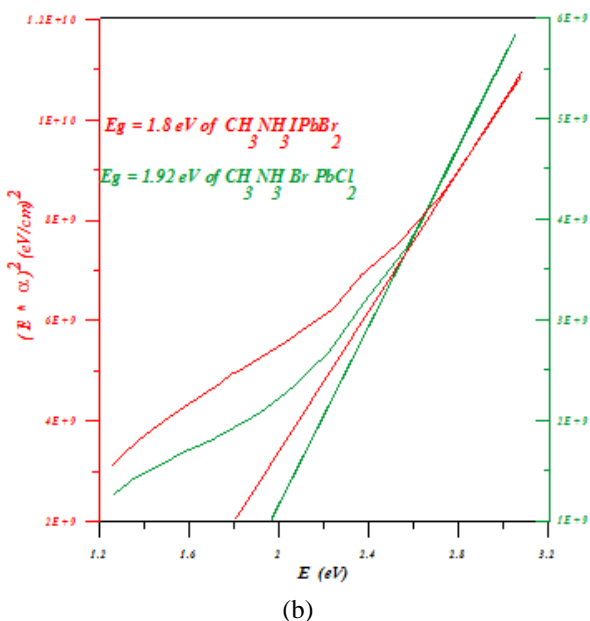
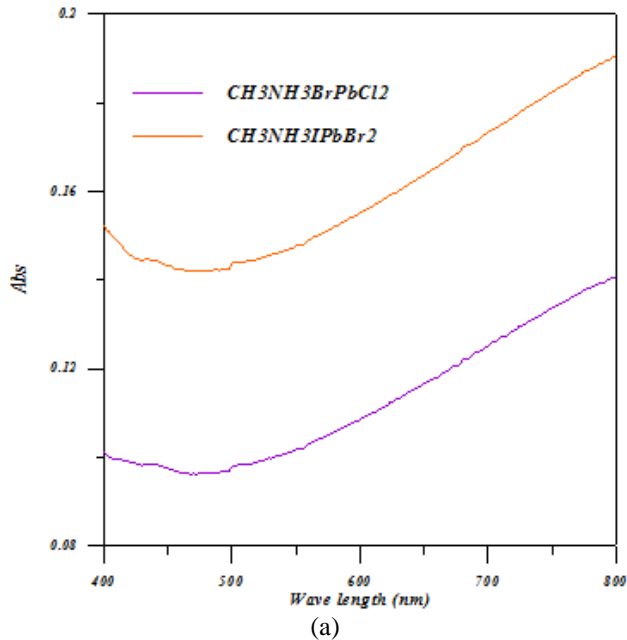
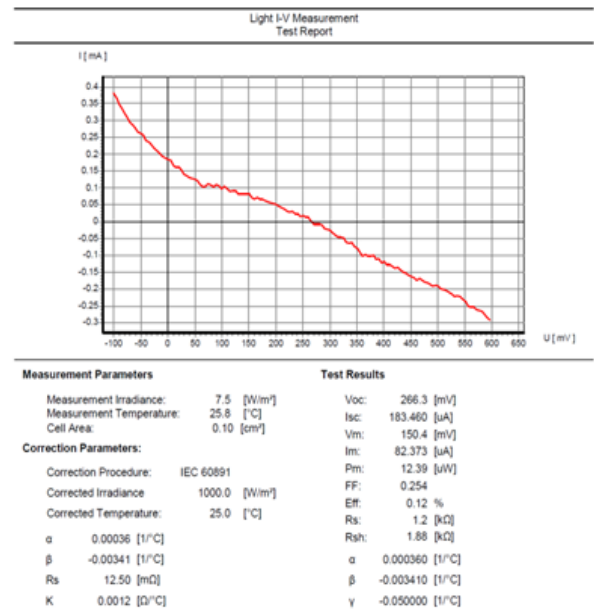
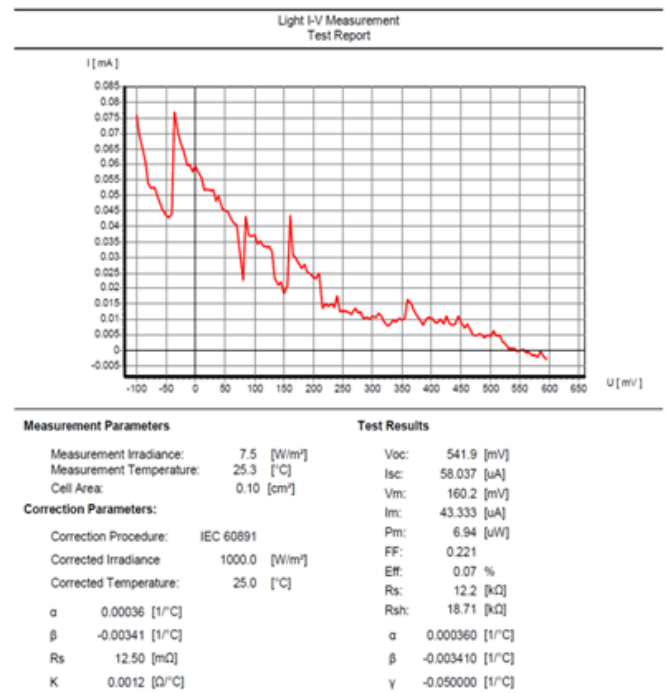


Fig 5a. depicts absorption of Visible light of the $CH_3NH_3IPbBr_2$ and $CH_3NH_3BrPbCl_2$ films. (b) explain energy gap of these films.



(a)



(b)

Fig 6a. I-V curve of OPSC has $CH_3NH_3IPbBr_2$ as absorption layer of device. (b). I-V curve of OPSC has $CH_3NH_3BrPbCl_2$ as absorption layer of device.

I-V curve of OPSC have best PCE to the device employed $CH_3NH_3IPbBr_2$ as absorption layer depicted in test report as shown in fig.6(a). Measurement is carried out under 1 sun illumination ($AM1.5G, 100 \text{ mW/cm}^2$), active area of solar cell is 0.1 cm^2 and sweeping voltages in the scan-direction with a scan rate of $s = 50 \text{ mV/s}$. Fig.6 (b) is the test report which depicted I-V curve of device employed $CH_3NH_3BrPbCl_2$ as absorption layer. Measurement is tested at the same conditions as the fig.6(a). We observed increased the short current circuit to the device employed mixed halide ($X = Br$ and I) $CH_3NH_3IPbBr_2$ as absorption layer and increased open voltage circuit to the device employed mixed halide ($X = Br$ and Cl) $CH_3NH_3BrPbCl_2$ as absorption layer as shown as in the figure (6)

Conclusions

In summary, the OPSCs which employed the perovskite materials of $\text{CH}_3\text{NH}_3\text{IPbBr}_2$ or $\text{CH}_3\text{NH}_3\text{BrPbCl}_2$ with Al_2O_3 scaffold as harvester light and absorption layer have been successfully fabricated. We obtained the best efficiency is (PCE = 0.12 %) for (FTO/ TiO_2 / $\text{CH}_3\text{NH}_3\text{IPbBr}_2$ perovskite with Al_2O_3 scaffold /CuI/Al electrode) device . We observed that PCE is increased when increased the absorption and decreased band gap energy of pervskite layer of OPSCs. We observed increased the short current circuit to the device employed mixed halide of (X = Br and I) as absorption layer and increased open voltage circuit to the device employed mixed halide of (X = Br and Cl) as absorption layer of devices.

References

1. Park, N.-G., "Organometal perovskite light absorbers toward a 20% efficiency lowcost solid-state mesoscopic solar cell.", *J. Phys. Chem. Lett.* 4, 2423–2429 (2013).
2. A. Kojima, K. Teshima, Y. Shirai, and T. Miyasaka, "Organometal halide perovskites as visible-light sensitizers for photovoltaic cells," *J. Am. Chem. Soc.* 131, 6050–6051 (2009).
3. Huawei Zhou, Yantao Shi, Qingshun Dong , Hong Zhang, Yujin Xing, Kai Wang, Yi Du, and Tingli Ma," Hole-Conductor-Free, Metal-Electrode-Free $\text{TiO}_2/\text{CH}_3\text{NH}_3\text{PbI}_3$ Heterojunction Solar Cells Based on a Low-Temperature Carbon Electrode", [dx.doi.org/10.1021/jz5017069](https://doi.org/10.1021/jz5017069) | *J. Phys. Chem. Lett.* 2014, 5, 3241–3246.
4. Jiandong Fan, Baohua Jia, and Min Gu," Perovskite-based low-cost and high-efficiency hybrid halide solar cells",*Vol. 2, No. 5 / October 2014 / Photon . Res.*
[http : //dx.doi.org/10.1364/-PRJ.2.000111](http://dx.doi.org/10.1364/-PRJ.2.000111).
5. L. Vasylechko, A. Senyshyn, and U. Bismayer, "Perovskite-Type Aluminates and Gallates. In K.A. Gschneidner, Jr., J.-C.G. Bünzli and V.K. Pecharsky, editors": *Handbook on the Physics and Chemistry of Rare Earths*, Vol. 39, Netherlands: North-Holland, 2009, pp. 113-295. ISBN: 978-0-444-53221-3 © Copyright 2009 Elsevier B.V. North-Holland.
6. Aqel Mashot Jafar, Mahdi Hasan Suhail ,Falah Mustafa Al-Attar and Mohammd K. Kalaf ," Organolead halide perovskite solar cells", 32nd European Photovoltaic Solar Energy Conference and Exhibition, pp(1296-1302), 2016, DOI:10.4229EUPVSEC2016-3DV.2.18.
7. Lioz Etgar," Semiconductor Nanocrystals as Light Harvesters in Solar Cells", *Materials* Vol. 6, (2013) 445-459.
8. Aqel M. Jafar, Mahdi H. Suhyl, Falah I. Mustafa," Organolead Iodide Perovskite Solar Cells (OPSC)", *AASCIT Journal of Energy*. Vol. 2, No. 6, 2015, pp. 81-87.
9. Aqel Mashot Jafar, Kiffah Al-Amara , Farhan Lafta Rashid and Ibrahim Kaïttan Fayyadh," Fabrication and Characterization of Fluorine-Doped Tin Oxide Transparent Conductive Nano-Films", *Elixir Nanotechnology* 65A , (2013) 20107-20111, www.elixirpublishers.com (Elixir International Journal).
10. D. Priante, I. Dursun, M. S. Alias, D. Shi, V. A. Melnikov, T. K. Ng, O. F. Mohammed, O. M. Bakr, and B. S. Ooi," The recombination mechanisms leading to amplified spontaneous emission at the truegreen wavelength in $\text{CH}_3\text{NH}_3\text{PbBr}_3$ perovskites", *Applied Physics Letters* 106, (2015) 081902.
11. Simone Guarnera, Antonio Abate, Wei Zhang, Jamie M. Foster, Giles Richardson, Annamaria Petrozza, and Henry J. Snaith., "Improving the longtermstability of perovskite solar cellswith a porous Al_2O_3 buffer layer," *The Journal of Physical Chemistry Letters*, vol. 6, no. 3, pp. 432–437, 2015.
12. Belen Suarez, Victoria Gonzalez-Pedro, Teresa S. Ripolles, Rafael S. Sanchez, Luis Otero, and Ivan Mora-Sero ," Recombination Study of Combined Halides (Cl, Br, I) Perovskite Solar Cells", [dx.doi.org/10.1021/jz5006797](https://doi.org/10.1021/jz5006797) | *J. Phys. Chem. Lett.* 2014, 5, 1628–1635.